TÜBİTAK

Turkish Journal of Physics

http://journals.tubitak.gov.tr/physics/

Research Article

Turk J Phys
(2016) 40: 201 – 208
© TÜBİTAK
doi:10.3906/fiz-1509-18

Crystal dynamics of zinc chalcogenides III: an application to ZnTe

Jay Prakash DUBEY[1,*], **Raj Kishore TIWARI**[2], **Kripa Shankar UPADHYAYA**[3], **Pramod Kumar PANDEY**[1]

[1]Department of Physics, Pandit Shambhu Nath Shukla Government Post Graduate College, Shahdol Affiliated to Awadhesh Pratap Singh University, Rewa, Madhya Pradesh, India

[2]Department of Physics, Government New Science College, Rewa Affiliated to Awadhesh Pratap Singh University, Rewa, Madhya Pradesh, India

[3]Department of Physics, Nehru Gram Bharati University, Allahabad, Uttar Pradesh, India

Received: 15.09.2015 • **Accepted/Published Online:** 24.03.2016 • **Final Version:** 01.12.2016

Abstract: We report the results of a theoretical study on phonon dispersion curves (PDCs) along the three principal symmetry directions, Debye temperature variation, combined density of states (CDS) curves, two-phonon Raman/IR peaks, and anharmonic elastic properties (third order elastic constants and their pressure derivatives) of ZnTe. This new van der Waals three-body force rigid shell model (VTRSM) incorporates the effect of van der Waals interactions and three-body interactions into the rigid shell model of zinc blende structure, where the short range interactions are operative up to the second neighbors. Our results are in good agreement with the available measured data for zinc telluride. It is concluded that this VTRSM will be equally applicable to study the above properties of other zinc blende structure solids.

Key words: Lattice dynamics, van der Waals interactions, Debye temperature variation, combined density of states curve, Raman spectra, zinc telluride

PACS No: 63.20.-e, 65.40.Ba, 78.30.-j

1. Introduction

The van der Waals three-body force rigid shell model (VTRSM) has been quite successful in explaining phonon dispersion curves, harmonic and anharmonic elastic constants, Debye temperature variation, combined density, cohesive energy, two phonon IR and Raman spectra, and numerous other physical properties. This crystal ZBS is promising for numerous experimental and theoretical investigations. These models, particularly neutron scattering, reported phonon dispersion curves for IIB–VIA and theories able to explain these results correctly. The theoretical models have been used in two categories: (i) the rigid ion model involves the ion rigidity hypothesis and (ii) the shell model involves ionic polarizability. Both models have been utilized for studying phonon dispersion in these compounds such as valence shell model (VSM) [1], ultrasonic pulse-echo (UPE) [2], rigid ion model (RIM) [3], valence force field model (VFFM) [4], bond charge model (BCM) [5], and others [6–10].

The above information encouraged us to include (i) the effect of VDWI and (ii) TBI in the framework of RSM where short range interactions are effective up to the second neighbors. Our new VTRSM has 14 parameters, i.e. four TBI parameters, b, ρ, f(r_0), and $r_0 f'(r_0)$; six nearest and the next nearest neighbor

*Correspondence: jpdubebl@yahoo.com

short-range repulsive interaction parameters, A_{12}, B_{12}, A_{11}, B_{11}, A_{22}, and B_{22}; two distortion polarizabilities of negative and positive ions, d_1 and d_2; and two shell charges of the negative and positive ions, Y_1 and Y_2, respectively. They can be deduced with the help of measured values of elastic constants, dielectric constants, electronic polarizabilities, and van der Waals coupling coefficients. This model has been applied to study the lattice dynamics of zinc chalcogenides (ZnS, ZnSe, ZnTe). In this communication, we are mainly concerned with the crystal dynamics of zinc telluride (ZnTe). Experimental data are given on ZnTe for phonon dispersion curves [1], harmonic and anharmonic elastic constants [2], Debye temperature variation [11–15], and two-phonon Raman [16] and IR spectra [17]. The first-order Raman spattering of ZBS-type crystal of two features corresponds to the transverse optic (TO) and longitudinal optic (LO) zone-center phonon modes. The second order Raman scattering of ZnTe, the total wave vector $\vec{q} = 0$ by the combinations of phonons, provides additional information on phonon mode frequencies at critical points near the edge of the first Brillouin zone. The formalism of our model VTRSM has been given [18,19].

2. Computations

The values of the input data given by Lee [2], Jai Shankar et al. [20], Berlin Court et al. [21], and Kunc et al. [22] and model parameters are shown in Table 1. The values of A_i, B_i, and C_i were calculated from the knowledge of b and ρ; the values of various orders of derivatives are $f(r_0)$ and van der Waals coupling coefficients [23]. The values of VDW coefficients used by us in the present study have been determined using SKV method [24] and Lee's [2] approach as suggested by Singh and Singh [25] and reported by Sharma and Verma [23]. Thus our model parameters are [b, ρ, $f(r_0)$, $r_0 f'(r_0)$, A_{12}, A_{11}, A_{22}, B_{12}, B_{11}, B_{22}, d_1, d_2, Y_1, and Y_2]. The VDW values are shown in Table 2. Our model parameters of VTRSM used to compute the phonon spectra for ZnTe allowed 48 nonequivalent wave vectors in the first Brillouin zone. The frequencies along the high symmetry [q00], [qq0], and [qqq] directions were plotted against the wave vector to obtain phonon dispersion curves (PDCs). These curves were compared with those measured by means of the coherent inelastic neutron scattering technique [1]; especially TA modes are very different not only from ours but also from RIM calculations of Camacho et al. [26] (Figure 1). Since the neutron scattering experiments provide us with very few data for the symmetry directions, we also computed CDS and the Debye temperature variation for the complete description of the frequencies for the Brillouin zone.

The complete phonon spectra were used to compute the combined density of states CDS, $N(\upsilon_j + \upsilon_{j'})$ corresponding to the sum modes $(\upsilon_j + \upsilon_{j'})$ following the procedure of Smart et al. [27]. A histogram between $N(\upsilon_j + \upsilon_{j'})$ and $(\upsilon_j + \upsilon_{j'})$ was plotted and smoothed out as shown in Figure 2. These curves show well defined peaks that correspond to two-phonon Raman scattering and IR absorption spectra. These CDS peaks were compared with the assignments calculated and are shown in Table 3. The Debye temperature variation for ZnTe given in the literature [11–15] and those calculated by us using the VTRSM are compared in Figure 3. The measured values of TOEC by Prasad [28] were compared with values of Sorgel and Scherz [29] and are shown in Table 4. The pressure derivatives of SOEC were also calculated and compared with those calculated by Dinesh et al. [30] and measured by Lee [2] (Table 5).

3. Results and discussion

3.1. Phonon dispersion curves

From Figure 1, our phonon dispersion curves for ZnTe agree well with measured data reported by Vagelatos et al. [1] at room temperature. It is evident from the PDCs that our predictions using the present VTRSM

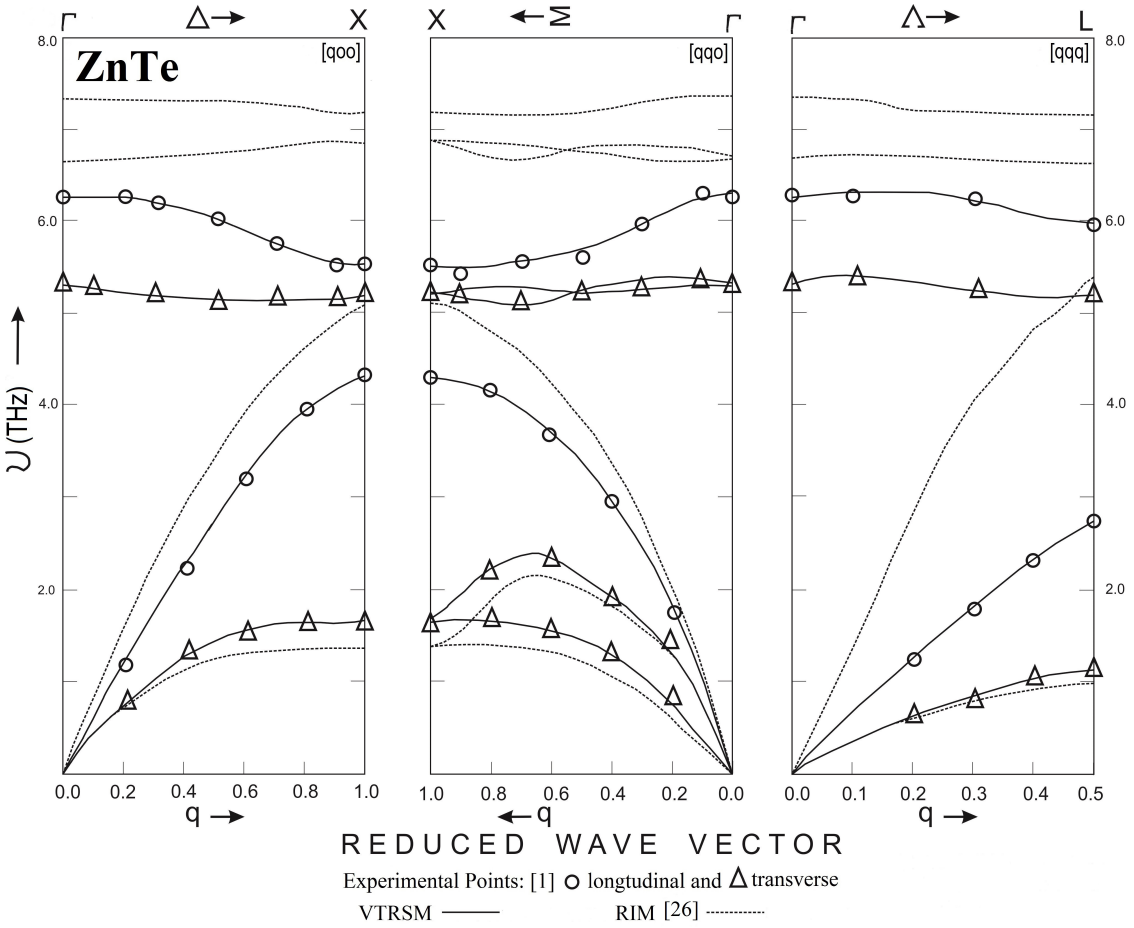

Figure 1. Phonon dispersion curves for ZnTe at room temperature.

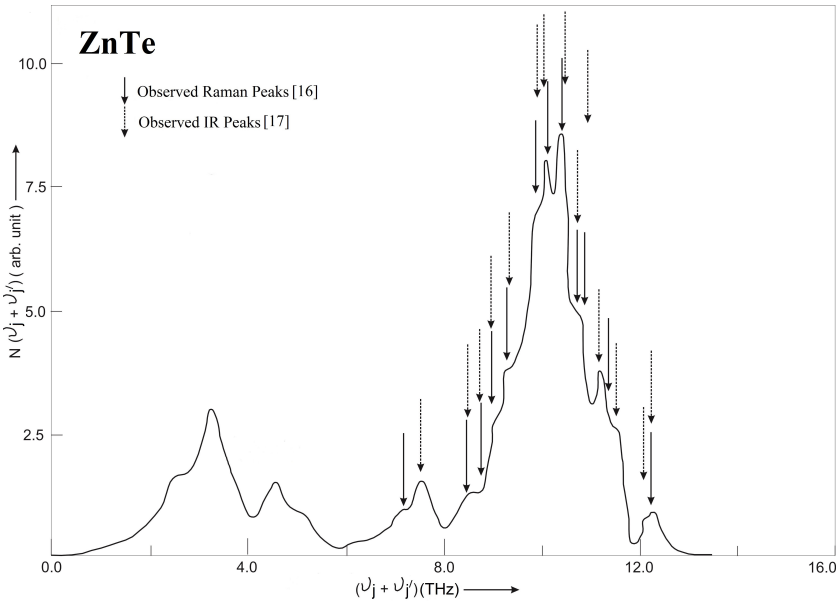

Figure 2. Combined density of states curve for ZnTe.

Table 1. Input data and model parameters for ZnTe [C_{ij} and B (in 10^{11} dyne/cm^2), υ (in THz), r_0 (in 10^{-8} cm), α_i (in 10^{-24} cm^3), b (in 10^{-12} erg), ρ (in 10^{-8} cm)].

Input data		Model parameters	
Properties	Values	Parameters	Values
C_{11}	7.13[a]	b	1.2800
C_{12}	4.07[a]	ρ	0.5260
C_{44}	3.12[a]	$f(r_0)$	–0.2100
B	5.08[a]	$r_0 f'(r_0)$	0.1058
r_0	2.64[b]	A_{12}	15.8583
$\upsilon_{LO}(\Gamma)$	6.20[c]	B_{12}	–5.2804
$\upsilon_{TO}(\Gamma)$	5.30[c]	A_{11}	154.0597
$\upsilon_{LO}(L)$	5.96*	B_{11}	–31.0613
$\upsilon_{TO}(L)$	5.11*	A_{22}	–2.6291
$\upsilon_{LA}(L)$	2.70*	B_{22}	–9.5200
$\upsilon_{TA}(L)$	1.44*	d_1	0.3076
α_1	1.14[d]	d_2	3.2223
α_2	8.50[d]	Y_1	–1.8486
ε_0	7.18[e]	Y_2	–1.3157

* Extrapolated values from [1].

[a]-(Lee [2]); [b]- (Berlin Court et al. [21]); [c]- (Vagelatos et al. [1]); [d]- (Shankar et al. [20]) and [e]- (Kunc et al. [22]).

Table 2. Van der Waals interaction coefficients for ZnTe (C_{ij} and C in units of 10^{-60} erg cm^6 and d_{ij} and D in units of 10^{-76} erg cm^8).

Parameters	Numerical values
C_{+-}	314
C_{++}	72
C_{--}	1684
d_{+-}	202
d_{++}	28
d_{--}	1365
C	2070
D	982

are better than those by using RIM [26]. Our model successfully explained the dispersion of phonons along the three high symmetry directions. From Figure 1 and Table 6, it is clear that there are deviations of 17.42% along LO(Γ), 25.58% along TO(Γ), 29.23% along LO(X), 29.75% along TO(X), 19.58% along LA(X), 23.46% along TA(X), 19.32% along LO(L), 26.44% along TO(L), 94.74% along LA(L), and 16.83% along TA(L) from the experimental results. From RIM, deviations are 17.42% along LO(Γ), 25.58% along TO(Γ), 29.41% along LO(X), 30.13% along TO(X), 23.46% along TA(X), and 95.49% along LA(L) and from VTRSM no % deviation along LO(Γ), no % deviation along TO(Γ), 0.18% along LO(X), 0.38% along TO(X), no % deviation along TA(X), and 0.75% along LA(L). From Table 6 it is clear that the VTRSM has very small deviation from the experimental data. Our model, VTRSM, has 94.74% improvement over RIM due to inclusion of TBI and VDWI coefficients. Thus, our VTRSM has better agreement with the experimental data than RIM [26].

Table 3. Assignments for the observed peak positions in combined density of states in terms of selected phonon frequencies at Γ, X, and L critical points for ZnTe.

CDS peaks (cm^{-1})	Raman active			Infrared active		
	Observed Raman peaks (cm^{-1}) [16]	Present study		Observed IR peaks (cm^{-1}) [17]	Present study	
		Values (cm^{-1})	Assignments		Values (cm^{-1})	Assignments
87	.....	89	LA-TA(X)	.....	.....	.....
108	.....	108	2TA(X)	.....	.....	.....
153	.....	140	LO-TA(Δ)	.....	.....	.....
170	.....	170	LA+TA(Δ)	.....	170	LA+TA(Δ)
240	240	236	2LA(Δ)	.....	236	2LA(Δ)
253	.....	244	LO+TA(Δ)	253	244	LO+TA(Δ)
282	282	286	2LA(X)	282	286	LO+LA(L)
290	290	290	TO+LA(Δ)	289	290	TO+LA(Δ)
300	300	.....	.....	302	.....	.....
310	310	310	LO+LA(Δ)	313	310	LO+LA(Δ)
330	329	326	LO+LA(X)	332	.....	.....
340	340	344	2TO(Δ)	337	344	2TO(Δ)
348	349	346	2TO(X)	351	.....	.....
357	358	356	LO+TO(X)	359	.....	.....
.....	364	364	LO+TO(Δ)	.....	364	LO+TO(Δ)
373	.....	366	2LO(X)	374	.....	.....
.....	.....	.....	.....	380	.....	.....
383	.....	394	2LO(L)	387	.....	.....
403	.....	.....	.....	403	.....	.....
410	412	414	2LO(Γ)	410	414	2LO(Γ)

Table 4. Third order elastic constants (in the unit of 10^{11} dyne/cm^2) for ZnTe.

Property	Present study	Experimental results [28]	Other theoretical results [29]
C_{111}	–69.2	–70.7	–49.2
C_{112}	–09.6	–12.1	–30.1
C_{123}	–45.9	–41.2	–0.87
C_{144}	15.8	18.3	–0.81
C_{166}	–23.6	–21.7	–13.9
C_{456}	–25.3	–22.9	–0.36

Table 5. Values of pressure derivatives of SOEC (dimensionless) for ZnTe.

Properties	Values			
	Present study	Experimental [2]	Other [29]	Other [31]
dK'/dP	5.12	5.04	5.16	4.60
dS'/dP	–0.44	–0.08	–0.44	–0.53
dC'_{44}/dP	0.62	0.45	0.95	2.92

Table 6. Comparison of frequencies from various sources (Γ, X, and L points) for ZnTe.

Points	Branches	Expt. [1]	RIM [26]			Present study			% Improvement over (RIM) (a ∼ b)
			Value (THz)	(±) Deviation	% (a)	Value (THz)	(±) Deviation	% (b)	
Γ (000)	LO	6.20	7.28	1.08	17.42	6.20	0.00	0.00	17.42
	TO	5.30	6.63	1.33	25.58	5.30	0.00	0.00	25.58
X (100)	LO	5.51	7.13	1.62	29.41	5.50	0.01	0.18	29.23
	TO	5.21	6.78	1.57	30.13	5.19	0.02	0.38	29.75
	LA	4.29	5.14	0.85	19.81	4.30	0.01	0.23	19.58
	TA	1.62	1.24	0.38	23.46	1.62	0.00	0.00	23.46
L (.5.5.5)	LO	5.90	7.06	1.16	19.66	5.92	0.02	0.34	19.32
	TO	5.18	6.57	1.39	26.83	5.20	0.02	0.39	26.44
	LA	2.66	5.20	2.54	95.49	2.68	0.02	0.75	94.74
	TA	1.07	0.86	0.21	19.63	1.10	0.03	2.80	16.83

3.2. Third order elastic constants (TOEC), pressure derivatives of second order elastic constants (SOEC)

Our calculations on TOEC are reported in Table 4 and compared with measured data of Prasad [28] on TOEC of ZnTe and the theoretical results of Sorgel and Scherz [29]. Further, pressure derivatives of SOEC for ZnTe were also compared with the calculated results of Dinesh et al. [30] and Khenata et al. [31], and measured data of Lee [2] as shown in Table 5. The results are in good agreement.

3.3. Combined density of states

The present model is capable of predicting the two-phonon Raman/IR spectra [16,17]. The results of these investigations for CDS peaks are presented in Figure 2. The theoretical peaks are in good agreement with both observed Raman/IR spectra for ZnTe. The assignments made by critical point analysis are shown in Table 3. The interpretation of Raman/IR spectra achieved from both CDS approach and critical point analysis is quite satisfactory. This explains that there is an excellent agreement between the experimental data and our theoretical results.

3.4. Debye temperature variation

From Figure 3, our study shows better agreement with the measured data from the literature [11–15] and the theoretical results reported by Vagelatos et al. [1] using VSM. To conclude, we can say that our model gives a better interpretation of the Debye temperatures variation for ZnTe.

4. Conclusion

The inclusion of VDWI with TBI influenced both the optical branches and the acoustic branches. Another striking feature of the present model is the excellent reproduction of almost all branches. Hence the prediction of PDC for ZnTe using VTRSM may be considered more satisfactory than from other models [26]. The basic aim of the study of two-phonon Raman/IR spectra is to correlate the neutron scattering and optical measured data of ZnTe. In this paper, we have systematically reported phonon dispersion curves, combined density of states, Debye temperature variation, and a part of the harmonic and anharmonic properties of ZnTe. On the basis of overall discussion, it is concluded that our VTRSM is adequately capable of describing the crystal dynamics of

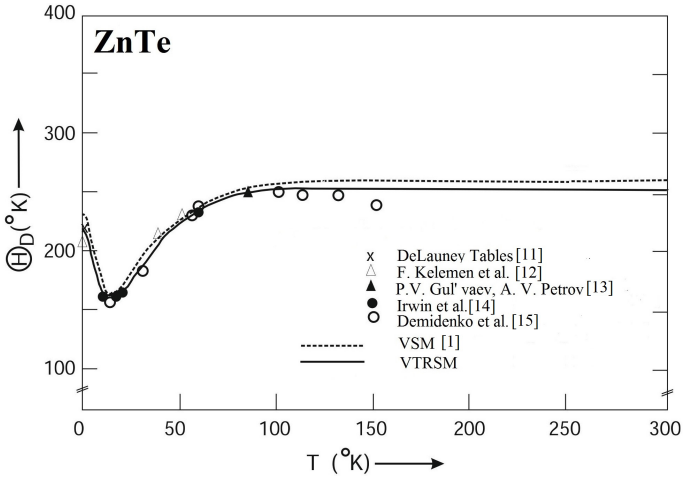

Figure 3. Debye characteristics temperatures Θ_D (°K) as a function of temperature T for ZnTe.

ZnTe. This model has also been applied equally well to study the crystal dynamics of other compound of this group, ZnS and ZnSe.

Acknowledgments

The authors are very grateful to Dr. A. N. Pandey, Ex. Reader and Head, Department of physics, K. N. Govt. P. G. College, Gyanpur, Bhadohi (U.P.), India for many useful discussions, and the computer center, B. H. U., Varanasi, for providing computational assistance. One of us, Mr. J. P. Dubey, is also thankful to Dr. Devendra Pathak, Vice chancellor, Dr. K. N. Modi University Newai, Rajasthan, India, for his encouragement.

References

[1] Vagelatos, N.; Wehe, D.; King, J. *J. Chem. Phys.* **1974**, *60*, 3613-3618.

[2] Lee, B. H. *J. Appl. Phys.* **1970**, *41*, 2988-2990.

[3] Talwar, D. N.; Vandevyver, M.; Kunc, K.; Zigone, M. *Phys. Rev. B* **1981**, *24*, 741-753.

[4] McMurry, H. L.; Solbrig, A. W.; Boytter, J. K.; Noble, C. *J. Phys. Chem.* **1967**, *28*, 2359.

[5] Rajput, B. D.; Browne, D. A. *Phys. Rev. B* **1996**, *53*, 9052-9058.

[6] Lee, G. D.; Lee, M. H.; Ihm, J. *Phys. Rev. B* **1995**, *52*, 1459.

[7] Kirin, D.; Lukacevic, I. *Phys. Rev. B* **2007**, *75*, 172103.

[8] Yeh, C. Y.; Lu, Z. W.; Froyen, S.; Zunger, A. *Phys. Rev. B* **1992**, *46*, 10086.

[9] Tan, J. J.; Ji, G. F.; Chen, X. R. *Commun. Theor. Phys. (Beijing, China)* **2010**, *53*, 1160-1166.

[10] Cote, M.; Zakharov, O.; Rubio, A.; Cohen, M. L. *Phys. Rev. B.* **1997**, 55, 13025.

[11] DeLaunnay, J. *J. Chem. Phys.* **1954**, *22*, 1676.

[12] Kelemen, F.; Niculescu, D.; Cruceanu, E. *Phys. Status Solidi* **1965**, *11*, 865-872

[13] Irwin, J. C.; LaCombe, J. *J. Appl. Phys.* **1974**, *45*, 224.

[14] Gul'yaer, P. V.; Petrov, A.; Sov, V. *Phys. Solid State* **1959**, *1*, 330-334.

[15] Demidenko, F. A.; Maltsev, A. K. *Izv. Akad. Nauk SSSR Neorg. Mater.* **1969**, *5*, 158-160.

[16] Irwin, J. C.; LaCombe, J. *Appl. Phys.* **1970**, *41*, 1444.

[17] Narita, S.; Harada, H.; Nagasaki, K. *J. Phys. Soc. (Japan)* **1967**, *22*, 1176.

[18] Dubey, J. P.; Tiwari, R. K.; Upadhyaya, K. S.; Pandey, P. K. *Turk. J. Phys.* **2015**, *39,* 242-253.

[19] Dubey, J. P.; Tiwari, R. K.; Upadhyaya, K. S.; Pandey, P. K. *IOSR Journal of Applied Physics* **2015**, 7, 67-75.

[20] Shankar, J.; Sharma, J. C.; Sharma, D. P. *Ind. J. Pure Appl. Phys.* **1977**, *5*, 811-820.

[21] Berlin Court, D.; Jaffe, H.; Shiozawa, L. R. *Phys. Rev.* **1963**, *129*, 1009-1017.

[22] Kunc, K.; Balkanski, M.; Nusimovici, M. A. *Phys. Status Solidi (b)* **1975**, *72*, 249-260.

[23] Sharma, U. C.; Verma, M. P. *Phys. Status Solidi (b)* **1980**, *102*, 487-494.

[24] Slater, J. C.; Kirkwood, J. G. *Phys. Rev.* **1931**, *37*, 682-697.

[25] Singh, R. K.; Singh, S. *Phys. Status Solidi (b)* **1987**, *140*, 407-413.

[26] Camacho, J.; Loa, I.; Cantarero, A.; Syassen, K. *J. Phys., Condens. Matter* **2002**, *14*, 739-757.

[27] Smart, C.; Wilkinson, G. R.; Karo, A. M.; Hardy, J. R. In *Lattice Dynamics*; Wallis, R. F., Ed.; Pergamon Press: Oxford, UK, 1965.

[28] Prasad, O. H.: PhD, Osmania University, Hyderabad, India, 1978.

[29] Sorgel, J.; Scherz, U. *Eur. Phys. J.* **1998**, B 5, 45-52.

[30] Varshney, D.; Sharma, P.; Kaurav, N.; Singh, R. K. *Bull. Mat. Sci.* **2005**, *28*, 651-661.

[31] Khenata, R.; Bouhemadou, A.; Sahnoun, M.; Reshak, A. H.; Baltache, H.; Rabah, M. *Comp. Mat. Sci.* **2006**, *38*, 29-38.